TAMPERE UNIVERSITY OF TECHNOLOGY

Computational Model for Simulating Multifocal Imaging in Optical Projection Tomography

Citation
Koskela, O., Belay, B., Pursiainen, S., Figueiras, E., & Hyttinen, J. (2017). Computational Model for Simulating Multifocal Imaging in Optical Projection Tomography. In *Mathematics in Imaging 2017* [MTu1C.3] Optical Society of America. https://doi.org/10.1364/MATH.2017.MTu1C.3

Year
2017

Version
Peer reviewed version (post-print)

Link to publication
TUTCRIS Portal (http://www.tut.fi/tutcris)

Published in
Mathematics in Imaging 2017

DOI
10.1364/MATH.2017.MTu1C.3

Copyright
© 2017 Optical Society of America. Users may use, reuse, and build upon the article, or use the article for text or data mining, so long as such uses are for non-commercial purposes and appropriate attribution is maintained. All other rights are reserved.

Take down policy
If you believe that this document breaches copyright, please contact cris.tau@tuni.fi, and we will remove access to the work immediately and investigate your claim.

Download date:18.10.2019

Computational model for simulating multifocal imaging in optical projection tomography

Olli Koskela[1], Birhanu Belay[1], Sampsa Pursiainen[2], Edite Figueiras[3], Jari Hyttinen[1]

1) BioMediTech Institute and Faculty of Biomedical Sciences and Engineering, Tampere University of Technology, Tampere, Finland

2) Department of Mathematics, Tampere University of Technology, Tampere, Finland

3) International Iberian Nanotechnology Laboratory, Braga, Portugal

olli.koskela@tut.fi

Abstract: We present a computational model describing the blurring of particles with respect to focal distance in 3D optical imaging. The model can be used to improve reconstructions in optical projection tomography.

OCIS codes: 100.6950, 170.6900.

1. Introduction

Optical projection tomography (OPT) [1] is often referred as the optical equivalent of X-ray computed tomography. In transmission OPT a set of projections are taken in series of angular steps from light transmitted through the sample. It has been applied in developmental biology for studies of zebra fish embryo anatomy in 3D environment [2,3]. Recently it has been shown to be a practical tool in hydrogel characterization as well [4, 5]. Different to X-ray imaging, OPT has limited depth of field: only objects at or close to the focal plane are in focus. The further the object is from focal plane, more blurry it is captured in the detector.

To address the limited depth of field, variety of techniques have been used [6–8]. One easily implemented is multifocal imaging [2]. In multifocal imaging multiple projections with different focal distances from each projection angle are acquired and fusioned into single all-in-focus image. The study showed improvement in OPT projection quality, but also noted no added benefit when using iterative reconstruction technique with multifocal imaging. All-in-focus fusion methods have been studied in more depth as a computer vision problem [9, 10]. Multifocal imaging has strong potential in cell imaging but it is unclear how to choose correct all-in-focus method for the application at hand.

In this work we present a computational model that can be used to numerically study the characteristics of different all-in-focus methods and further their effects on the tomographic reconstructions from multifocal data.

2. Materials and methods

2.1. Forward model and all-in-focus fusion methods

Standard Radon transform in tomography under parallel beam geometry consists of ray-transform through applying Beer-Lambert law to y-direction in the numerical phantom $P \in [1,r]^3 \subset \mathbf{R}^3$ (phantom of resolution r in the compact support subspace). This assumes everything within the sample to be equally focused as they are in X-ray imaging. In simulations, point spread function and noise of the detector are applied to data afterwards.

We include a simple step to model a focusing lens that captures particles accurately in a specific distance — in the focal plane of the lens — and the further the particle is from the focal plane, the more blurry it is captured. Our model is based on convolution of the phantom and focusing kernel matrix $F \in \mathbf{R}^2$ in x and z coordinates in each rotational position before ray-transform. Note here that convolution is orthogonal to ray-transform. Matrix $F \in \mathbf{R}^{r \times p}$ describes the focusing properties of the optical lens system and is of same the height as the phantom. Width of F depends on parameters. It is possible to have also separate F_x and F_z in case the components are different.

In this comparison we used two all-in-focus fusion algorithms, namely extended depth of field (eDOF) from [2], and maximum variance fusion method. Maximum variance fusion method computes the variance of each pixel in each projection image in a given window. For fusion image the pixel value in the original images giving the maximum variance is chosen.

In simulations we used a phantom with three inclusions (attenuation coefficient 1) in a medium (attenuation coefficient 0.1). For focusing kernel we used Bessel function of the first kind and of order 0. All of the computations were performed in MATLAB.

2.2. *Experimental materials and methods*

Stromal cells (PA6 cells) embedded on hydrogel biomaterial were imaged using in-house built OPT system [4]. The samples were inserted inside fluorinated ethylene propylene (FEP) tubes with 3 mm outside diameter (Adtech Polymer Engineering) and immersed in a transparent cuvette (Hellma Anaytics) filled with water for bright-field imaging.

In OPT the sample was illuminated using a white LED with a telecentric backlight illuminator (Edmund) for bright-field imaging. The light transmitted through the sample was detected by 5x infinity corrected objective (Thorlabs) with a numerical aperture (NA) of 0.14, an iris diaphragm (Thorlabs) and a 200 mm tube lens (Mitutoyo). The projection images were collected with a sCMOS camera (ORCA-Flash 4.0, Hamamatsu). Multifocal images were acquired by translating the sample along the optical axis. For each angle of projection, a total of 23 images were recorded with 100 μm scanning distance through the sample. The images were acquired over 360 degrees with a rotational step size of 0.9 degrees.

3. Results and conclusions

The presented model is capable of simulating focusing in optical imaging systems with different properties that can be given in the kernel F. The properties of the kernel depend on the application and can be e.g. Gaussian distributions or Bessel functions. The latter was used in this study as it provides physically more relevant properties: the halo effect around the cells. Example is shown in the figure 1.

Multifocal imaging provides more details from samples, figures 2a–2e depicts this. Cells in the sample are on different distances from the detection objective and thus not always in focus due to the limited depth of field of the objective lens. By scanning through the sample it is possible to capture accurately cells at different distances. Using an all-in-focus fusion algorithm these details can be projected into one image. Once this is done for all projection angles, tomographic reconstructions can be computed applying inverse Radon-transform and all the details should be visible in the reconstructions as well. Two examples of all-in-focus fusions are shown in figures 2g and 2h.

However, all-in-focus fusion algorithms cannot be used just by plug-and-play approach. As the examples show, output can be drastically different depending on the algorithm and parameters used, and these differences will be further propagated to tomographic reconstructions as well. In this comparison the maximum variance fusion method seems to provide more application suitable output.

The presented model shows potential as a theoretical analysis method for the multifocal instrumentation and can be used to model the physical parameters of the focusing. Multifocal imaging has strong potential to capture more detail from the sample and if correct computational methods are chosen, those details can be produced to reconstructions as well. Analysis of computational methods, their limits and cross method dependencies are needed.

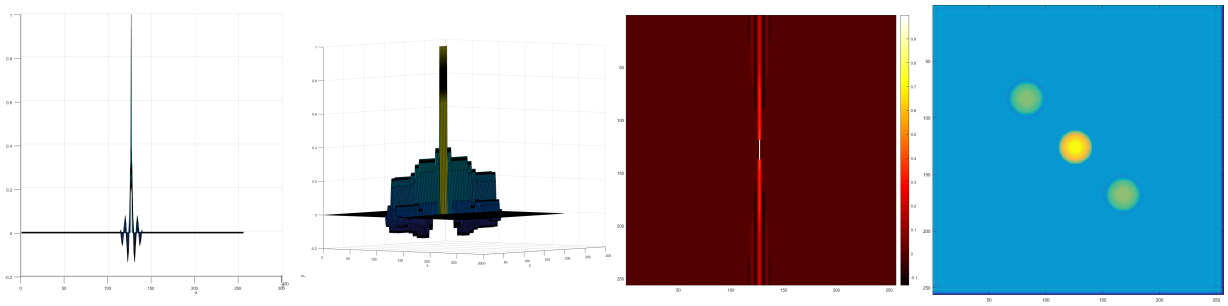

(a) (b) (c) (d)

Fig. 1: Focusing kernel with Bessel function: a) cross sections in x direction, b) 3D view of the profile, and c) view from the top in xy coordinates. d) Projection image from a simulated phantom using Bessel kernel.

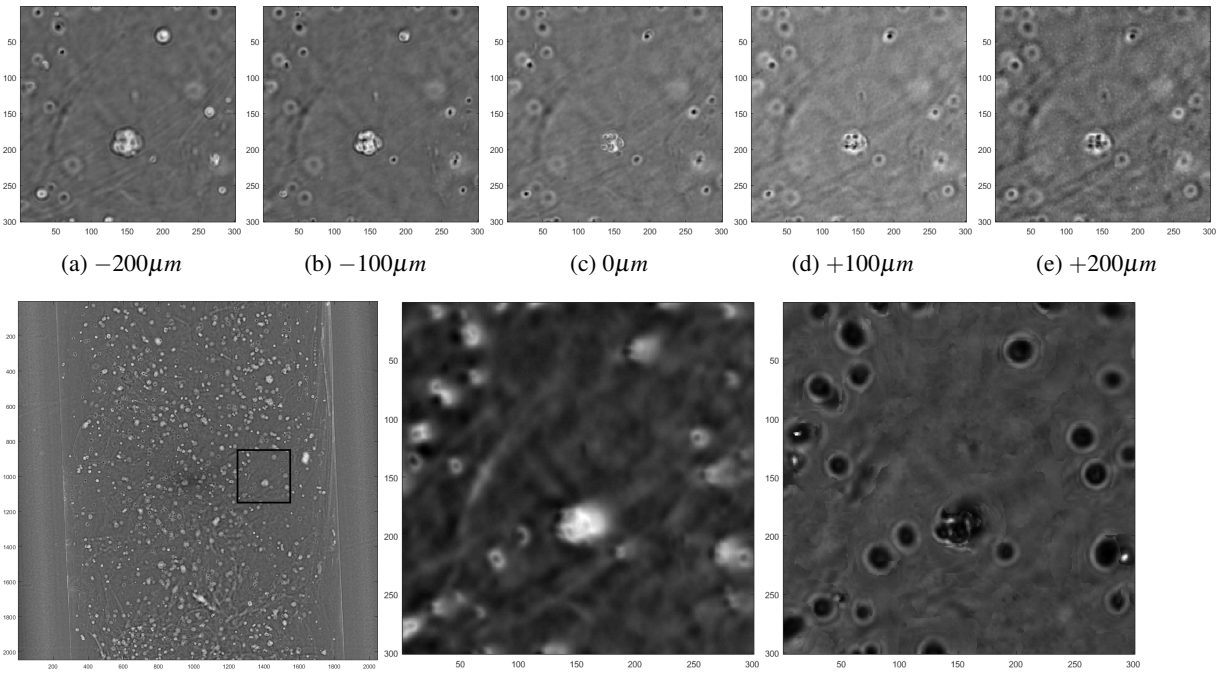

(a) $-200\mu m$ (b) $-100\mu m$ (c) $0\mu m$ (d) $+100\mu m$ (e) $+200\mu m$

(f) (g) (h)

Fig. 2: a–e) Raw data close-up example showing a cell cluster in focus (c) and its behavior out-of-focus. OPT images of a cell sample from one angle: f) raw projection, g) close-up of eDOF fusion of 23 projection images, and h) close-up maximum variance fusion image from 23 projection images. All close-ups are from the square box in f.

References

1. J. Sharpe, U. Ahlgren, P. Perry, B. Hill, A. Ross, J. Hecksher-Sørensen, R. Baldock, and D. Davidson, "Optical projection tomography as a tool for 3d microscopy and gene expression studies," Science **296**, 541–545 (2002).
2. A. Bassi, B. Schmid, and J. Huisken, "Optical tomography complements light sheet microscopy for in toto imaging of zebrafish development," Development **142**, 1016–1020 (2015).
3. J. Sharpe, "Optical projection tomography as a new tool for studying embryo anatomy," Journal of anatomy **202**, 175–181 (2003).
4. E. Figueiras, A. M. Soto, D. Jesus, M. Lehti, J. Koivisto, J. Parraga, J. Silva-Correia, J. Oliveira, R. Reis, M. Kellomäki *et al.*, "Optical projection tomography as a tool for 3d imaging of hydrogels," Biomedical optics express **5**, 3443–3449 (2014).
5. A. M. Soto, J. T. Koivisto, J. E. Parraga, J. Silva-Correia, J. M. Oliveira, R. L. Reis, M. Kellomaki, J. Hyttinen, and E. Figueiras, "Optical projection tomography technique for image texture and mass transport studies in hydrogels based on gellan gum," Langmuir **32**, 5173–5182 (2016).
6. L. Chen, N. Andrews, S. Kumar, P. Frankel, J. McGinty, and P. M. French, "Simultaneous angular multiplexing optical projection tomography at shifted focal planes," Optics letters **38**, 851–853 (2013).
7. Q. Miao, J. Hayenga, M. G. Meyer, T. Neumann, A. C. Nelson, and E. J. Seibel, "Resolution improvement in optical projection tomography by the focal scanning method," Optics letters **35**, 3363–3365 (2010).
8. L. Chen, S. Kumar, D. Kelly, N. Andrews, M. J. Dallman, P. M. French, and J. McGinty, "Remote focal scanning optical projection tomography with an electrically tunable lens," Biomedical optics express **5**, 3367–3375 (2014).
9. S. Pertuz, D. Puig, M. A. Garcia, and A. Fusiello, "Generation of all-in-focus images by noise-robust selective fusion of limited depth-of-field images," IEEE Transactions on Image Processing **22**, 1242–1251 (2013).
10. S. Li, X. Kang, L. Fang, J. Hu, and H. Yin, "Pixel-level image fusion: A survey of the state of the art," Information Fusion **33**, 100–112 (2017).